https://doi.org/10.5194/egusphere-2026-3326
Preprint. Discussion started: 19 June 2026


# Lithium isotopes reveal impaired ion transport in tropical corals exposed to high $pCO_2$

Nathalie Vigier[a,*], Fanny Thibon[a,f], Riccardo Rodolfo Metalpa[b], Maryline Montanes[a], Arbia Jouini[a], Laurent Counillon[c], Mallorie Poet[c], Malcolm McCulloch[d], Clément Tanvet[b,e], Philippe Télouk[f], Steeve Comeau[a,d]

[a]Laboratoire d'Océanographie de Villefranche (LOV), CNRS, Sorbonne Université, 06230 Villefranche-sur-Mer, France

[b]Centre IRD Nouméa, UMR ENTROPIE (IRD, Université de la Réunion, Université de la Nouvelle-Calédonie, Ifremer), Nouméa 98848, New Caledonia

[c]Université Côte d'Azur, CNRS, Laboratoire de Physiologie Cellulaire et Moléculaire (LP2M), 06107 Nice, France

[d]Oceans Graduate School, The University of Western Australia, Crawley 6009, Western Australia, Australia

[e]Univ Brest, CNRS, IRD, Ifremer, LEMAR, F-29280 Plouzané, France

[f]Laboratoire de Géologie de Lyon – Terre Planètes Environnement (LGL-TPE), CNRS, ENS-UCBL-UJM, 69007 Lyon, France

- *Corresponding author:* nathalie.vigier@imev-mer.fr

https://doi.org/10.5194/egusphere-2026-3326
Preprint. Discussion started: 19 June 2026


**Abstract**

Ocean acidification, driven by rising atmospheric $CO_2$, threatens the ability of corals to build their skeletons by reducing their capacity to maintain an elevated pH at the calcification site ($pH_{cf}$), a process essential for calcium carbonate precipitation. Boron isotopes have commonly been used to show that the response of $pH_{cf}$ to ocean acidification is highly species-specific. However, the physiological mechanisms underlying this variability remain poorly understood. Recently, lithium (Li) isotopes have been used to trace the activity of ionic transport involved in cellular pH regulation and calcification (e.g. $H^+$, $Na^+$ and $Ca^{2+}$), and may therefore help resolve these mechanisms. Here, we investigate multiple coral species from Tutum Bay (Papua New Guinea), a natural $CO_2$ seep system creating pH gradients (mean $pH_T$ = 7.66 at seeps vs. 8.01 at control sites) analogous to future ocean acidification scenarios. Our results show a relationship between seawater pH, calcifying fluid chemistry, and lithium isotopic composition. Corals exposed to low seawater pH exhibit significantly altered $\delta^7Li$ values relative to colonies from the control site, with some species becoming enriched in $^7Li$ (up to 2‰) as $pH_{cf}$ declines. This isotopic shift is consistent with reduced efficiency of $Na^+/H^+$ exchangers (NHEs), active transporters that preferentially incorporate the lighter $^6Li$ isotope under optimal conditions but may become less effective under elevated proton concentrations. By linking Li isotopes to calcifying-fluid chemistry, these results provide geochemical evidence that ocean acidification may disrupt ionic regulation in corals and that Li isotopes can help to resolve biogeochemical controls of carbonate-systems.

**Keywords**: lithium isotopes, ocean acidification, ionic transport, coral calcification

https://doi.org/10.5194/egusphere-2026-3326
Preprint. Discussion started: 19 June 2026


## Introduction

Scleractinian corals first appeared during the mid-Triassic (~237 Ma) and are foundational species in marine ecosystems and coral reefs. Coral reefs are now largely threatened by ocean acidification (OA) resulting from rapid increase of atmospheric $CO_2$ levels (Hoegh-Guldberg et al. 2017) and coral responses to ocean acidification are highly species-specific (Okazaki et al. 2017; Comeau et al. 2013; Fabricius et al. 2011). Their skeletal geochemistry, including Mg/Ca, Li/Mg ratios, boron isotopes ($\delta^{11}B$), and B/Ca ratios, has been widely used to study the impact of ocean acidification and global warming on their physiology (McCulloch et al. 2017; Guillermic et al. 2021), as well as for reconstructing past oceanic conditions (Clarke et al. 2017; Fallon et al. 2003; Mitsuguchi et al. 1996; Quinn and Sampson 2002; Zeebe and Wolf-Gladrow 2001). For instance, Li/Mg ratios in coral skeletons are recognized as a proxy for past seawater temperatures (Case et al. 2010; Cuny-Guirriec et al. 2019; D'Olivo et al. 2018; Montagna et al. 2014; Fowell et al. 2016) and boron isotopes and B/Ca are used to investigate the links between seawater environmental conditions and coral growth (e.g. McCulloch et al. 2017).

Coral colonies comprise interconnected polyps bound by a coenosarc overlying an aragonitic skeleton. Calcification occurs in the extracellular calcifying medium (or calcifying fluid, CF), a specialized microenvironment located between the skeleton and the calcifying cell layer (Figure 1). Boron isotope geochemistry ($\delta^{11}B$ and B/Ca), confocal microscopy, and microprobes have been employed to demonstrate that some coral species maintain pH and dissolved inorganic carbon (DIC) concentrations in their calcifying fluids at levels higher than surrounding seawater (e.g. Venn et al. 2013). However, this physiological mechanism can be affected by variations of multiple environmental conditions (Comeau et al. 2017; Foster and Rae 2016; Holcomb et al. 2014; McCulloch et al. 2017). Although boron isotopes provide key constraints on calcifying-fluid chemistry (pH and DIC concentration), they do not directly

https://doi.org/10.5194/egusphere-2026-3326
Preprint. Discussion started: 19 June 2026


resolve the ion-transport processes that sustain pH regulation and carbonate precipitation under ocean acidification. In contrast, the activity of key ion transporters ($Ca^{2+}$, $Na^{+}$, $H^{+}$) is less known while they regulate internal pH, creating and maintaining conditions essential for skeletal formation (Figure 1) (Orr et al. 2005; Rollion-Bard et al. 2015; Venn et al. 2022).

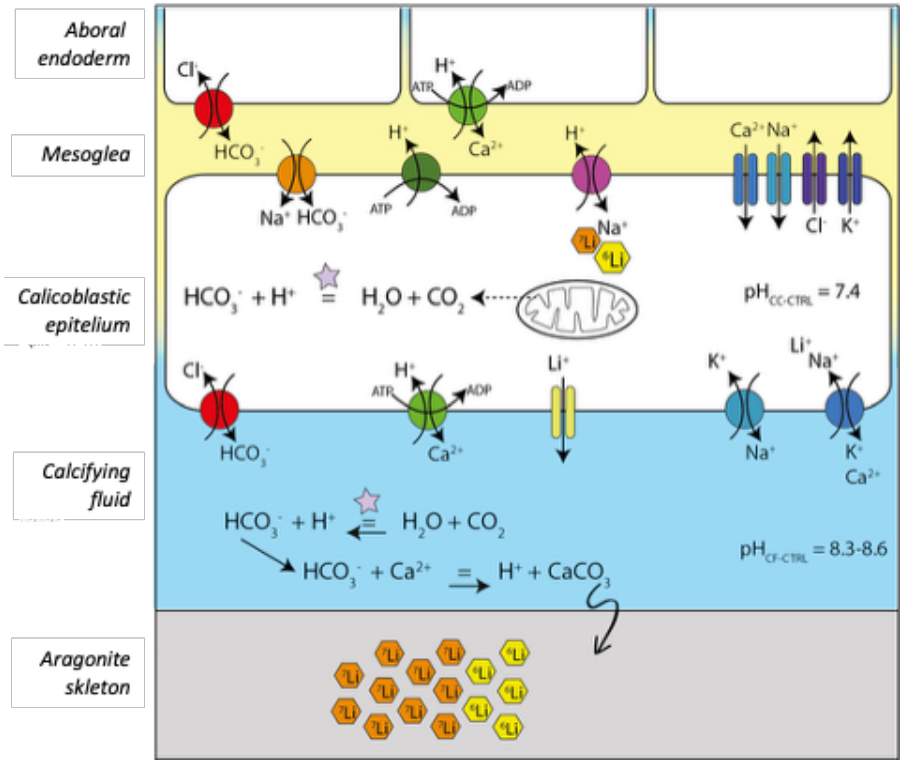


**Figure 1:** Schematic diagram of coral tissue cross-sections from aboral endoderm (top) to aragonite skeleton (bottom), and associated ion transport processes controlling calcifying fluid composition (for full cross-section, see figure S1). Individual cells are represented by white rectangles. Ion transporters (symporters, antiporters, or pumps) are in colored circles, while passive ion channels are in colored rectangles. The stars represent the action of carbonic anhydrase. Heavy $^{7}Li$ isotopes are in orange hexagons, and light $^{6}Li$ isotopes, in yellow hexagons. Kinetic transport systematically favors the light $^{6}Li$ isotope (Poet et al. 2023).

https://doi.org/10.5194/egusphere-2026-3326
Preprint. Discussion started: 19 June 2026


Despite their importance, the effects of environmental stressors on ionic transport remain poorly understood and bridging this knowledge gap becomes critical. Because $Li^+$ can behave as a $Na^+$ analogue in biological systems, lithium isotopes, largely sensitive to kinetic effects because of their high relative mass difference, can provide indirect information on Li fractionating ion-transport pathways involved in pH regulation and calcification, including $Na^+/H^+$ exchangers (Poet et al. 2023; Thibon et al. 2021a; Vigier et al. 2015).

Naturally acidified sites such as volcanic $CO_2$ seeps and semi-enclosed lagoons provide unique opportunities to investigate the effects of ocean acidification (OA) over time scales that cannot be replicated in laboratory experiments. Here, we used one such natural laboratory, Tutum Bay (Ambitle Island, Papua New Guinea), where seawater pH fluctuates around mean values similar to those predicted for the global ocean by the end of this century (pH ~7.7–7.8), to study the physiological responses of tropical shallow-water scleractinian corals using geochemical approaches. We compared similar species collected from two sites with contrasting carbonate chemistry: (1) a low-pH site (mean $pH_T$ = 7.66) near $CO_2$ seeps, and (2) a control site with ambient seawater pH (mean $pH_T$ = 8.01). We then assessed lithium systematics ($\delta^7$Li, Li concentration, and Li/Mg ratios) to complement the boron geochemistry ($\delta^{11}$B and B/Ca) previously published by Comeau et al. (2022) for the same samples. We tested three hypotheses: (1) low seawater pH induces changes in lithium-based proxies such as Li/Ca, Li/Mg, and $\delta^7$Li; (2) these effects are species-specific; and (3) lower pH at the calcification site corresponds to greater Li isotopic alteration, indicating reduced activity of ionic transporters.

https://doi.org/10.5194/egusphere-2026-3326
Preprint. Discussion started: 19 June 2026


## 1. Materials and Methods

### 2.1 Environmental characterization and samples description

The biogeochemistry of seawater and gases released in Tutum Bay at Ambitle Island (New Ireland, Papua New Guinea) (Figure 2) has been extensively characterized (Pichler et al. 2019). The whole bay (low pH site) has a mean pH ranging from 7.6 to 7.7 and an approximately constant 30°C temperature year-round. The reduced seawater pH, and the resulting changes in carbonate chemistry, are driven by the continuous and substantial release of $CO_2$ from four main volcanic vents and seeps dispersed throughout the bay.

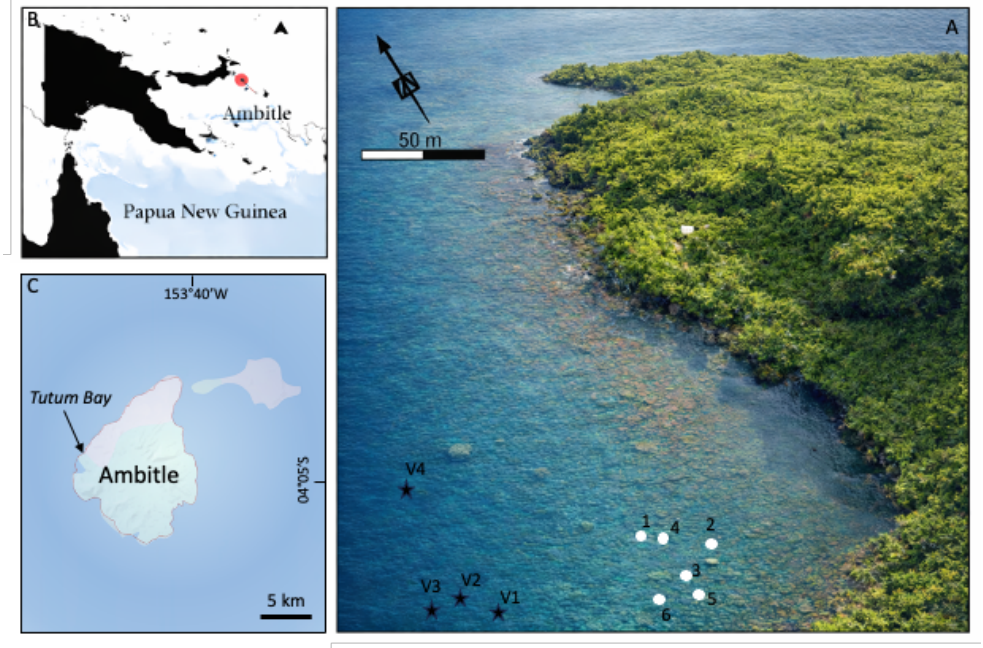


**Figure 2 :** Aerial picture of Tutum Bay (modified from Pichler et al. (2019)) showing the position of the stations 1-6 (white dots) where the pH was measured using SeaFETs during May 2018. Stars indicate the position of the four main massive vents. Ambient station (CTRL site) was around one mile south of Tutum Bay.

https://doi.org/10.5194/egusphere-2026-3326
Preprint. Discussion started: 19 June 2026


Between 2016 to 2018 the site was visited four times using the R/V Alis (e.g., Rodolfo-Metalpa 2018) and seawater $pH_T$ (in total scale) was measured during daily to weekly-cycles using SeaFET loggers (Sea-Bird Scientific, Bellevue, WA, USA) set to measure at 5-min intervals. Here, we utilize the environmental data collected during the fieldwork from 2016 and 2017 both at stations 1, 3-6 (Fig. 2; see also (Pichler et al. 2019) for a whole bay data assessment) and at a control site located 1.8 km south of the main seep, where corals were collected in May 2017.

Seawater temperature at both the seeps and control sites was measured from September 21, 2016 to May 23, 2017 by Hobo (Onset, Bourne, MA, USA) temperature loggers, logging at 5-min intervals and deployed at 3 m depth. Discrete seawater samples were also collected to measure total alkalinity. The gas composition of the seeps in Tutum Bay consisted of 93 to 98% $CO_2$, with minor amounts of nitrogen ($N_2$, 2 to 5%), methane ($CH_4$, < 2%), oxygen, (<1%), a trace of helium, but no traces of toxic sulfur compounds such as $H_2S$ (Pichler et al. 2019).

We sampled three fragments from three spatially separated (>10 m distance) corals both at $CO_2$ seep site and at a control site. The investigated species are either branching (*Acropora* sp1., *Acropora* sp2., *Pocillopora* c.f. *damicornis*), massive (*Galaxea fascicularis*, *Porites* sp.), foliated (*Montipora* sp., *Echinopora lamellosa*), or encrusting (*Psammocora* sp.) (Figs. 3 & S2). As shown in Figure 3, the surface-area to volume ratio (specific surface area) differed among species, from the massive and smooth *Porites* sp. to the fine lace built by *G. Fascicularis*.

Coral tissues were carefully removed on board using an air-pick in seawater and skeletons were dried at 40°C overnight. Corals were analyzed at the University of Western Australia for $\delta^{11}B$, B/Ca, and Li/Mg. Lithium extraction and purification were performed on the same specimens at the *Laboratoire d'Océanographie de Villefranche* (LOV, France).

https://doi.org/10.5194/egusphere-2026-3326
Preprint. Discussion started: 19 June 2026


147

148 **2.2. Calculation of calcifying pH and dissolved inorganic carbon**

149 We used the data and methods reported in Comeau et al. (2022) for the same samples and
150 report here a brief summary. Samples were first cleaned with mQ water, bleached for 24 h in
151 6.25 % NaClO to remove organic matter and dried for 48 h in a drying oven at 50°C. For
152 *Acroporidae* and *Pocilloporidae* genera, $\delta^{11}B$ and B/Ca were determined on a ~ 1 cm long piece
153 of skeleton from the tip of three branches for each of the three colonies analyzed that were
154 pooled together to smooth potential spatial differences. For massive corals (e.g., *Galaxea*), a
155 fragment of 0.5 $cm^3$ located ~ 0.5 cm below the surface was sampled. For *Montipora* sp. and
156 *Echinopora lamellosa*, a section of the skeleton close to the tip was sampled using cutting
157 pliers. The selected portions of skeletons were bleached for an additional 24 h in 6.25 % NaClO
158 and then rinsed three times with mQ water before drying for 48h at 50°C. The samples were
159 then crushed in a mortar with a pestle to powder.
160 In the clean laboratory of the Advanced Geochemical Facility for Indian Ocean Research
161 (AGFIOR, University of Western Australia), 10 mg of each coral aragonitic powder were
162 cleaned and then dissolved in 0.5 N $HNO_3$, from which a 10-ppm Ca aliquot was prepared for
163 trace element determinations. Boron was quantitatively separated on ion exchange columns
164 with B/Ca ratios determined on the same sub-aliquot of the solution used for trace-elements.
165 Boron isotope compositions are expressed in conventional delta notation relative to the boric
166 international standard (NBS951): $\delta^{11}B$ (‰) = ($^{11}B/^{10}B_{sample}$ / $^{11}B/^{10}B_{standard}$ -1)*1000. $\delta^{11}B$ was
167 measured on a NU II Multicollector Inductively Coupled Plasma Mass Spectrometer (MC-ICP-
168 MS). Measurements of the international carbonate standard JCP-1 (nominal value of 24.33 ±
169 0.11 ‰ (SE)) yielded a mean value of 24.43 ± 0.08 ‰ (mean ± SE, n = 10).

https://doi.org/10.5194/egusphere-2026-3326
Preprint. Discussion started: 19 June 2026


Based on similar B concentration and $d^{11}B$ in seawater for both sites (Comeau et al. 2022), $pH_{cf}$ was estimated from $\delta^{11}B$ using the calculations described by Trotter et al. (2011), as:

$$pH_{cf} = pK_B - \log\left[\frac{(\delta^{11}B_{SW} - \delta^{11}B_{carb})}{(\alpha_{(B3-B4)}\delta^{11}B_{carb} - \delta^{11}B_{SW} + 1000(\alpha_{(B3-B4)} - 1))}\right] \quad (1)$$

where $pK_B$ is the dissociation constant dependent on temperature and salinity, $\delta^{11}B_{sw}$ = 39.61 (Foster et al. 2010), and $\alpha_{(B3-B4)}$ is the boron isotopic fractionation factor for the pH dependent equilibrium of the borate ($B(OH)_4^-$) relative to the boric acid ($B(OH)_3$) species in the calcifying fluid, with a value of 1.0272 (Klochko et al. 2006). Furthermore, $[CO_3^{2-}]_{cf}$ can also be reconstructed using the equilibrium reaction of borate ion incorporation into carbonates (0.5 $CaCO_3$ + $B(OH)_4^-$ ↔ $Ca_{0.5}B(OH)_4$ + 0.5 $CO_3^{2-}$) (15,17,18). Knowing $pH_{cf}$ and $[CO_3^{2-}]_{cf}$, dissolved inorganic carbon concentration of calcifying fluid ($DIC_{cf}$) can be calculated using carbonate equilibrium equations:

$$DIC_{cf} = [CO_3^{2-}]_{cf} \times \left(1 + \frac{[H^+]}{K_2} + \frac{[H^+]^2}{K_1 + K_2}\right) \quad (3)$$

where $K_1$ and $K_2$ are equilibrium constants (first and second dissociation constants of carbonic acid, respectively).

### 2.3. Lithium isotopes measurements

Following the same strategy as for boron, coral samples were weighted and transferred into 5 mL clean centrifuge tubes. To remove external contamination, corals were leached for two days with $H_2O_2$ at ambient temperature. Afterwards, samples were rinsed with distilled water, dried at 60°C, and ground into a fine powder with an agate mill. Aliquots of 15 mg were transferred to 1.5mL centrifuge tubes. A second leaching procedure was performed with $HNO_3$

https://doi.org/10.5194/egusphere-2026-3326
Preprint. Discussion started: 19 June 2026


0.05N + $H_2O_2$ 10% for one day at ambient temperature to ensure the removal of residual organic matter, following the method of Bastian et al. (2018). After a rinse with distilled water, samples were dissolved with 0.5 mL of 1N HCl at ambient temperature for Li purification.

Seawater Li isotopic composition was also determined on seawater samples collected in the control site and ca. 50 m upstream the vents between the stations 1 to 6 (Figure 2). The sampling was done using 20 mL polypropylene vials, previously rinsed three times using filtered seawater (Whatman™ Puradisc CA syringe filters 0.45 µm). Samples were immediately poisoned with 20 µL saturated $HgCl_2$, and then sub-sampled in 1.5 mL tubes. Aliquots were dried up and taken up in 0.5 mL of 1N HCl before Li separation.

Lithium extraction and purification were operated according to Vigier et al. (2008) and to Jouini et al. (2026). The samples dissolved in 0.5 mL of 1N HCl were loaded on AG 50-X12 (200-400 mesh) cationic resin in 8.5 cm high Teflon columns. Li was eluted and purified with 1N HCl. This fraction was then dried down and re-dissolved in 0.05N $HNO_3$ before measurements.

The delta notation, expressed in per-mill (‰), is classically used for reporting the $^7Li/^6Li$ isotope ratio: $\delta^7Li_{sample}$ (‰) = $\left(\frac{\left(\frac{^7Li}{^6Li}\right)_{sample}}{\left(\frac{^7Li}{^6Li}\right)_{standard}} - 1\right) * 1000$ (see e.g. Burton and Vigier 2011).

Measurements of Li isotopic ratio were performed at the CNRS-INSU Facilities at Ecole Normale Supérieure de Lyon, using a MC-ICP-MS (Thermo-Fisher Neptune *Plus*). The instrument was set in dry plasma conditions and low-resolution mode (Bastian et al. 2018; Balter and Vigier 2014; Thibon et al. 2021b). The sample-standard bracketing method (using LSVEC reference material) was applied for instrumental mass bias correction. Analytical and total procedural blanks were negligible. The internal reproducibility was, on average, ± 0.04‰ (2σ). Precision (external reproducibility), estimated from 2 to 5 replicated measurements of 12 different samples, was ~0.3‰ (2SD). The entire procedure accuracy was checked by the

https://doi.org/10.5194/egusphere-2026-3326
Preprint. Discussion started: 19 June 2026


analyses of a biogenic calcium carbonate reference material (JCp-1, *Porites sp.* coral), with a mean $\delta^7Li$ value of 18.8 ± 0.6 ‰ (2 SE, n = 9) (Bastian et al. 2018).

Because the $\delta^7Li$ value of the seawater at the seeps site was lower than at the control site (by -2.3 ‰, see section 3.1.), direct comparison of coral isotopic compositions between both sites is not appropriate for assessing the pH effect. Therefore, we calculated the Li isotope fractionation at each site as the difference in Li isotopic composition ($\Delta^7Li$) between seawater (SW) and coral skeleton (carb): $\Delta^7Li = \delta^7Li_{carb} - \delta^7Li_{sw}$.

### 2.4. Relationship between lithium chemistry and carbonate chemistry

We used different approaches to evaluate potential relationships between carbonate chemistry and lithium isotopes. First, we explored this relationship at the specie level using mean value for $\delta^{11}B_{carb}$, $\delta^7Li_{carb}$, $Li_{carb}$, $Li/Mg_{carb}$, $Mg/Ca_{carb}$, $B/Mg_{carb}$, $B/Ca_{carb}$, $Li/Ca_{carb}$, $pH_{cf}$ and $DIC_{cf}$, for each species. These were based on n = 2 to 5 individual measurements, except for *Acropora* sp.1 and *Montipora* sp., for which only one sample was available. Non-parametric statistical tests were used because the assumptions of normality and homoscedasticity for the Li compositional and isotopic data were not met (using Q-Q plots and Residuals vs. Fitted plots). Mann-Whitney-Wilcoxon tests were used to compare median values between two observational series between seeps and control corals. Statistical analyses were performed using R software (R core Team 2017) using the function *wilcox.test*.

Relationships among quantitative variables were investigated using principal component analysis (PCA). PCA was performed using R software using the following variables: $pH_{cf}$, $DIC_{cf}$, $D^7Li$, $Li/Ca_{carb}$, $B/Mg_{carb}$, $B/Ca_{carb}$, and $Li_{carb}$.

https://doi.org/10.5194/egusphere-2026-3326
Preprint. Discussion started: 19 June 2026


## 3. Results

### 3.1. Seawater lithium and carbonate chemistry

As previously reported in the literature for this area (Comeau et al. 2022; Pichler et al. 2019; Bell et al. 2022; Biscerer et al. 2019; Geissler et al. 2021; Meunier et al. 2021) and in open access database (https://doi.pangaea.de/10.1594/PANGAEA.939651), mean seawater pH is lower at the seep site when compared to the control. In the seep area where corals were collected, seawater pH fluctuated between 7.47 and 7.80 $pH_T$ units ($5^{th}$ and $95^{th}$ percentile), corresponding to $\Omega_{arag}$ values of 2.03 - 3.95, $pCO_2$ values of 793-1863 µatm and DIC values of 2135 – 2276 µmol $kg^{-1}$ ($5^{th}$ and $95^{th}$ percentile). Seawater $pH_T$ remained between 7.6–7.8 ($pCO_2$ = 799 -1349 µatm) for 60% of the time, below 7.6 ($pCO_2$ < 1349 µatm) for 24% of the time, and above 7.8 ($pCO_2$ > 799 µatm) for 16% of the time. In contrast, the control site exhibited higher and more stable pH ($pH_T$ ~ 7.94 -8.06; $pCO_2$ ~ 376 – 530 µatm; $5^{th}$ and $95^{th}$ percentile), while DIC concentrations ranged from 1955 to 2029 µmol $kg^{-1}$ ($5^{th}$ and $95^{th}$ percentile). Mean ± SD seawater temperature measured from September 2016 to May 2017 were 30.61 ± 0.23 °C, and 30.76 ± 0.25 °C at the control and seeps site, respectively.

Several seawater samples collected at the control site yielded $\delta^7Li$ values and Li concentrations typical of the open ocean (31.5 ± 1.1‰ and 0.18 ± 0.01 mg $L^{-1}$, respectively). At the seep site, Li concentrations were more variable and slightly higher than the open ocean, although the difference was not statistically significant (0.24 ± 0.4 mg $L^{-1}$). The mean seawater $\delta^7Li$ value at the seep site was 29.2 ± 0.7‰, slightly but significantly lower than at the control site. This observation is consistent with a slight hydrothermal contribution at the seep site, as hydrothermal fluids are enriched in Li compared to the open ocean by more than two orders of magnitude (e.g. Verney-Carron et al. 2011).

https://doi.org/10.5194/egusphere-2026-3326
Preprint. Discussion started: 19 June 2026


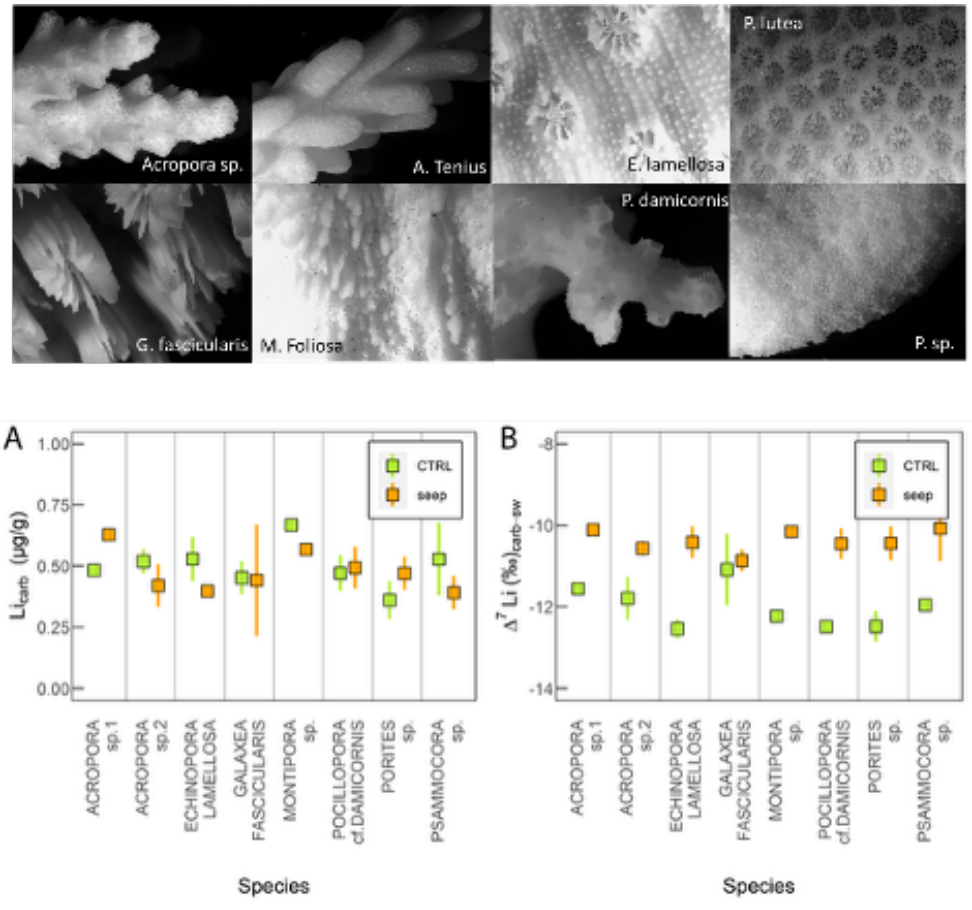


**Figure 3: (A)** Coral Li concentration (µg/g) and **(B)** Skeleton Li isotope composition $\delta^7Li_{carb}$ ( ‰) for each species collected at the control (CTRL, green) and seep sites (seep, orange). The squares are the means, and the error bars show the standard error ($2\sigma_n$). The species effect on Li concentration was observed to be small despite different skeleton morphologies and growth rates. **(C).** Coral aragonitic skeletons cleaned and analyzed in this study (using 10x binocular magnifier). The various structures and shapes highlight strong differences in biomineralization mode and rate.

Assuming that this fluid has a $\delta^7$Li typical of most marine hydrothermal fluids (8‰), and a Li content of 100 µg $mL^{-1}$ (Verney. et al. 2011), a contribution of 0.015 % of this fluid could explain the observed difference between the seep and the control Li isotopic signature. Due

https://doi.org/10.5194/egusphere-2026-3326
Preprint. Discussion started: 19 June 2026


to the strong contrast in Li concentration and isotopic signature between seawater and hydrothermal fluids, these data confirm that the contribution from hydrothermal fluid is minimal, consistent with previous observations that Ambitle seeps are primarily dominated by $CO_2$ gas (Pichler et al. 1999).

### 3.2. Coral calcifying fluid carbonate chemistry

A detailed description of the boron chemistry and estimated calcifying fluid carbonate chemistry is available in Comeau et al. (2022) and in Table S1. In brief, $\delta^{11}B$ ranged from 21.9 to 25.7 ‰ at the control site and from 20.7 to 24.5 ‰ at the seep site (Fig. S3). The difference in $\Delta^{11}B$ between seep and control sites varied from -2.8 ‰ for *E. lamellosa* to -0.3 ‰ for *Montipora sp*. (except for *G. fascicularis* showing a positive difference of 2.4‰), indicating that the effect of seawater pH on the skeleton $\delta^{11}B$ composition is specie- and site -specific (Fig. S2).

Calculated calcifying fluid $pH_{cf}$ ranged from 8.2 to 8.5 (Comeau et al. 2022) (Table S1). Although the average differences between sites for $pH_{cf}$ was not significant, the effects of seawater pH on $pH_{cf}$ was highly species specific. Some species displayed a marked decline in $pH_{cf}$ in response to low seawater pH while other were not much affected ($pH_{cf\text{-}VENT}$ - $pH_{cf\text{-}CTRL}$ range between -0.19 and -0.02).

$B/Ca_{carb}$ ranged between 445 µmol $mol^{-1}$ (*E. lamellosa* from the seep site) and 592 µmol $mol^{-1}$ (*G. fascicularis* from the seep site). As a result, estimated $DIC_{cf}$ ranged from 3468 to 4859 µmol.$kg^{-1}$, with no significant differences between sites when averaged across species. However, as for $pH_{cf}$, the response of $DIC_{cf}$ to low seawater pH was species specific.

https://doi.org/10.5194/egusphere-2026-3326
Preprint. Discussion started: 19 June 2026


### 3.3. Coral lithium chemistry

Lithium contents ranged from 0.36 ± 0.08 µg $g^{-1}$ in *Porites* sp. (2 SE, n = 5) to 0.67 µg $g^{-1}$ in *Montipora* sp. (n = 1), consistent with previously reported values for marine biogenic tissues (Bastian et al. 2018; Dellinger et al. 2018; Chen et al. 2023; Thibon et al. 2022). Lithium concentrations and Li/Ca ratio did not differ significantly between corals living under low pH conditions and those from control pH ($p > 0.05$). At the control site, mean $Li_{carb}$ was 0.50 ± 0.06 µg $g^{-1}$, ($2\sigma_n$, n = 8) whereas at the seeps site it was 0.48 ± 0.06 µg $g^{-1}$ ($2\sigma_n$, n = 8) (Figs. 4A & 3A). The molar ratios of Mg/Ca ranged from 4.1 to 5.9 × $10^{-3}$, and skeleton Li/Mg ratio ranged from 1.0 to 1.5 × $10^{-3}$. Both are comparable to values reported for various coral species (Table S1) (Montagna et al. 2014; Comeau et al. 2017; Bastian et al. 2018; Rollion-Bard et al. 2009; Dissart et al. 2012; Douville et al. 2010). Mean coral Li/Mg values at the seep and control sites were similar within uncertainties, averaging 1.32 ± 0.07 and 1.26 ± 0.08 mmol $mol^{-1}$ respectively (2 SE, n = 8).

Coral $\delta^7Li_{carb}$ values ranged from 18.3 ± 0.3 ‰ in *G. fascicularis* from the seeps site (2 SE, n = 2) to 20.4 ± 0.9 ‰ in *G. fascicularis* from the control site (2 SE, n = 3). $\delta^7Li_{carb}$ was systematically highly enriched in the light $^6Li$ isotope compared to the seawater values for all corals. These values are consistent with values published previously (from 17.1 ± 0.9 ‰ to 23.8 ± 0.9 ‰, Table S1), although isotopic data for corals remain scarce (Marriott et al. 2004a; Marriott et al. 2004b; Bastian et al. 2018; Rollion-Bard et al. 2009). The average seawater-coral Li isotope fractionation ($\Delta^7Li_{CTRL\text{-}sw} = \delta^7Li_{carb} - \delta^7Li_{sw}$) at the control site was -12.0 ± 0.4 ‰. At the seep site, $\Delta^7Li_{seep\text{-}sw}$ was slightly but significantly lower (-10.4 ± 0.2 ‰). Again this is in agreement with the literature as coral skeletons are generally enriched in $^6Li$ compared to seawater, resulting in negative isotopic fractionation (Marriott et al. 2004a; Marriott et al. 2004b; Bastian et al. 2018; Rollion-Bard et al. 2009). However, we observed here that the magnitude

https://doi.org/10.5194/egusphere-2026-3326
Preprint. Discussion started: 19 June 2026


of Li isotopic fractionation differed significantly between seeps and control sites (Wilcox. test, $p < 0.001$).

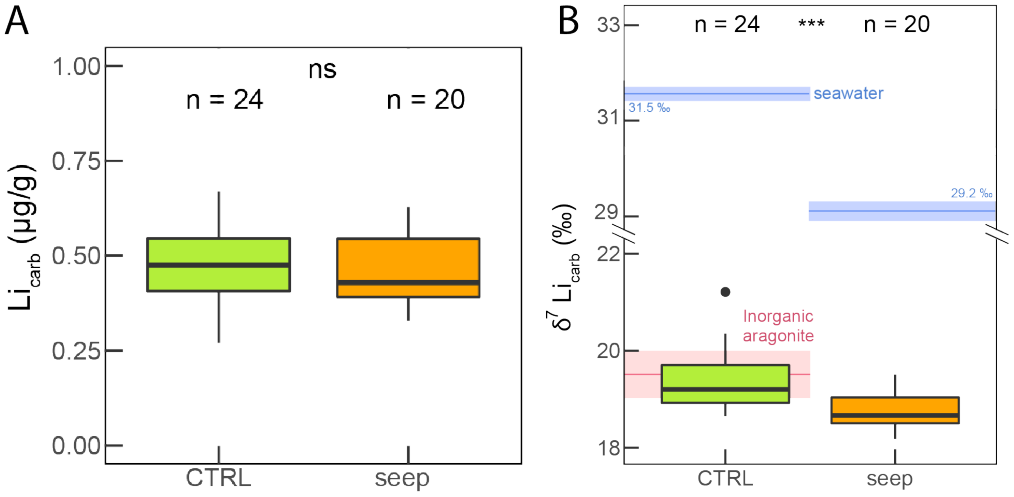


**Figure 4:** Box plots showing **(A)** the Li concentration (µg $g^{-1}$), **(B)** the skeleton Li isotope composition $\delta^7Li_{carb}$ (‰) of corals living under high $pCO_2$ seawater (seep) and ambient seawater at the (CTRL) site. Seawater $\delta^7Li$ values are added in blue for comparison. The numbers at the top of each box indicate the number of replicates. Asterisks show the significance of the Mann-Whitney-Wilcoxon tests used to observe differences between pairs of groups: ns (not significant) for $p > 0.05$, *** for $p < 0.001$). Outliers (> 1.5 Interquartile range) are plotted as black circles.

## 4. Discussion

Our results indicate that long-term exposure to naturally low seawater pH does not markedly alter coral Li concentrations or Li/Mg ratios, but is associated with significant changes in Li

https://doi.org/10.5194/egusphere-2026-3326
Preprint. Discussion started: 19 June 2026


isotope fractionation. Importantly, these isotopic changes are species-specific and covary with boron-derived estimates of calcifying-fluid chemistry, suggesting that $\delta^7$Li may record physiological differences in the regulation of ion transport and calcification under acidified conditions.

### 4.1. Biological and species effects on Li concentrations and Li isotopes

Despite slightly higher Li concentrations in the seawater at the seep site compared to the control site, Li concentrations in coral skeletons remains similar between sites. This suggests that biological processes internally regulate lithium uptake in corals, which is consistent with observations in other marine calcifying species (see Thibon et al. 2021c).

Additional evidence for biological control comes from the limited variability in Li partition coefficients among species, with $LogD_{Li}$ ranging from -3.38 to -3.26 (Table S1 and Fig. S5). This indicates that species, growth rate, and skeleton architecture play a limited role for this variable, in agreement with previous studies (Bastian et al. 2018) and SIMS chemical micro-analyses (Rollion-Bard et al. 2009). It is however striking that this range is one order of magnitude lower than the one determined for inorganic aragonite formed in the laboratory under similar conditions ($LogD_{Li}$ value between -2.37 and -2.52 at pH = 8.1-8.3, Chen et al. 2023), which strongly suggests a biological regulation of Li incorporation by scleractinian corals.

Coral $\delta^7$Li values also differ between cultured and naturally growing corals. The average $\delta^7Li_{carb}$ value displayed by cultured corals is lower (17.3 ± 0.2 ‰, 2 SE, n = 28, Bastian et al. 2018) than in corals living in natural conditions at Ambitle (19.5 ± 0.4 ‰, 2 SE, n = 24), despite experimental conditions mimicking at best natural environmental parameters, such as pH, salinity, DIC, temperature, and light intensity (although light was artificial). In addition, the $\delta^7$Li values of corals grown at the Ambitle control site ( 1.45 ‰ ) is twice that given by seven

https://doi.org/10.5194/egusphere-2026-3326
Preprint. Discussion started: 19 June 2026


363 species living in an aquarium fed by Mediterranean seawater (0.7 ‰, see Bastian et al. 2018).
364 This also indicates an "aquarium effect" potentially related to a biological regulation of lithium
365 that may be affected by experimental conditions.
366
367

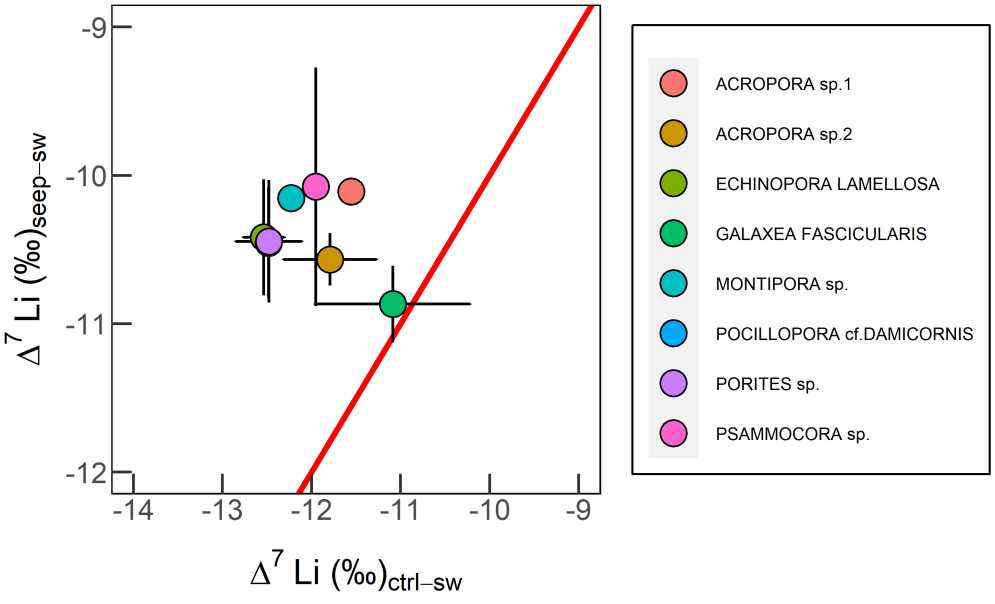


368 **Figure 5:** Coral skeleton Li isotope composition $\delta^7Li_{carb}$ (‰) at seep site *versus* control site.
369 Each purple dot represents the mean value for one coral species. Error bars in 2 SE ($2\sigma_n$), the
370 red line represents the identity line.
371
372

373 The influence of biological processes on Li isotopes can also be evaluated by comparing coral
374 skeletons with inorganic aragonite precipitated under similar conditions. At pH = 8.1, inorganic
375 aragonite exhibits a $\delta^7$Li of 19.2‰ ± 1.5‰ (±2 SE) (Chen et al. 2023). Relative to this reference,
376 an isotopic vital effect of -1.9‰ ± 1.2‰ (2 SE) is observed for scleractinian corals grown in
377 aquarium (Bastian et al. 2018), whereas corals from natural environments, including Jarvis

https://doi.org/10.5194/egusphere-2026-3326
Preprint. Discussion started: 19 June 2026


Island (Marriott et al. 2004ab) and the Ambitle control site, exhibit much smaller vital effects (about −0.4‰). This again suggests a biological influence on lithium isotopes in corals and highlight that studying corals sampled from their natural environment appears particularly relevant for Li isotopes.

Although Li concentrations and seawater–carbonate Li isotope fractionations vary only modestly among species at a given site, the response to acidified conditions differs significantly between species. For instance, low Li level coral species appear more sensitive to their environment since corals with high Li/Ca ratio exhibit smaller differences in $\delta^7Li_{carb}$ between the two sites (see Fig. S5). Because trace-element incorporation in biogenic carbonates is influenced by both environmental conditions and growth-related biological processes (Chen et al., 2023), these interspecific differences likely reflect contrasting physiological responses to low-pH conditions as corals experienced similar environmental conditions within sites.

### 4.2. Limited influence of pH on the coral Li/Mg temperature proxy

Previous studies have shown that coral Li/Mg ratios are negatively correlated with seawater temperature (Montagna et al. 2014; Stewart et al. 2020). The coral species analyzed here follow the established Li/Mg–temperature relationship of Montagna et al. (2014) and Stewart et al. (2013), with reconstructed temperatures closely matching *in situ* seawater temperatures at both seep and control sites (Figure 6). These results suggest that a seawater pH decrease of ~0.4 units does not substantially bias the coral Li/Mg temperature proxy at Tutum Bay.

In contrast to Li isotopes, Li/Mg ratios show only limited sensitivity to acidified conditions. Nevertheless, among corals from the seep site, Li/Mg is positively correlated with $pH_{cf}$ ($r = 0.58$), whereas no such relationship is observed at the control site (Table S2). This may indicate

https://doi.org/10.5194/egusphere-2026-3326
Preprint. Discussion started: 19 June 2026


that low-pH conditions influence Mg transport or incorporation into the calcifying fluid, although additional work is required to test this hypothesis.

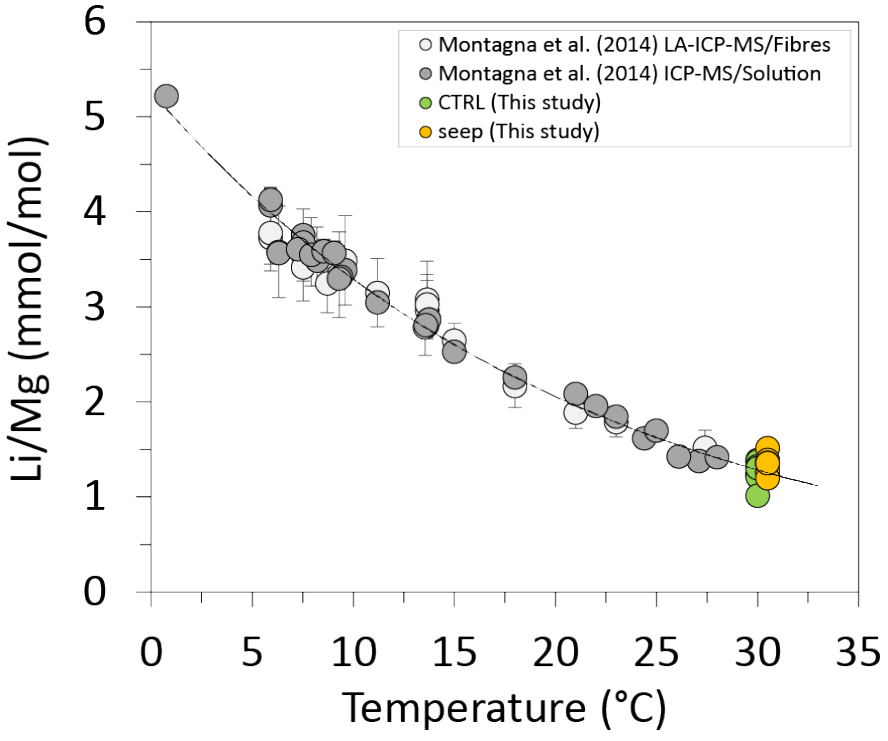


**Figure 6:** Corals $Li/Mg_{carb}$ ratios versus seawater temperature. Each circle corresponds to one coral individual. Data from Montagna et al. (2014) consist of *C. caespitosa, Acropora sp., Porites sp., L. pertusa, M. oculata,* and *F. impensum*, from various geographic origins (Mediterranean Sea, Atlantic, Pacific, and Southern Oceans), and cultured corals species *C. caespitosa*, and *Acropora sp*. Orange and green circles code from this study corals (Seep and CTRL respectively), *i.e., Acropora* sp1*., Acropora* sp2*., G. fascicularis, Porites* sp*., Montipora* sp*., E. lamellosa, Pasammocora* sp*.,* and *P.* cf. *damicornis*. Shadow areas underline the temperature range evaluated from $Li/Mg_{carb}$ under each condition.

https://doi.org/10.5194/egusphere-2026-3326
Preprint. Discussion started: 19 June 2026


### 4.3. Strong link between pH and lithium isotopes

Here we assess whether pH influences Li isotope fractionation during skeleton growth. Principal component analysis performed on seven quantitative variables ($pH_{cf}$, $DIC_{cf}$, $\delta^7Li_{carb}$, $Li/Ca_{carb}$, $B/Mg_{carb}$, $B/Ca_{carb}$, $Li_{carb}$) reveals that $pH_{cf}$ and $\delta^7Li_{carb}$ covary and together contribute to the separation between seeps and control corals (Fig. 7). This indicates that a decrease in seawater pH is associated, for several coral species, to changes in both the calcifying fluid pH and the skeleton Li isotope signature, suggesting a strong link between these parameters.

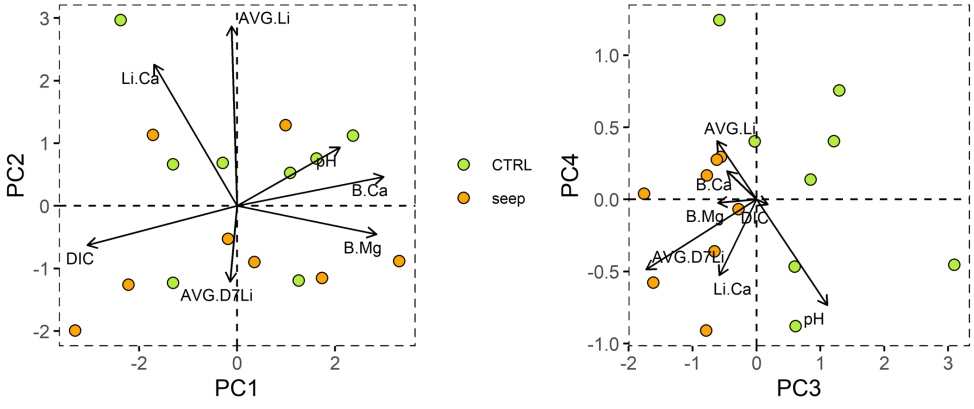


**Figure 7:** Results obtained with a PCA applied to coral skeleton parameters. PC3 and PC4 are for principal components 3 and 4 and represent 23 % of the variability of the dataset. Points are for individuals. Variable row length is proportional to their contribution to the principal components. Thus, $pH_{cf}$ and $\delta^7Li$ are the main variables that contribute to PC3 and PC4. Furthermore, PC3 and PC4 can discriminate seep and CTRL groups (*i.e.,* seep data plot mainly in the bottom left panel, and CTRL data plot mainly in the top right panel). Therefore, both groups can clearly be distinguished based on $pH_{cf}$ and $\delta^7Li$.

This relationship is further illustrated in Figure 8, where the difference in species $\delta^7Li_{carb}$ between the control and seeps sites ($\Delta^7Li_{seep\text{-}CTRL} = \delta^7Li_{carb\text{-}seep} - \delta^7Li_{carb\text{-}CTRL}$) is correlated to both

https://doi.org/10.5194/egusphere-2026-3326
Preprint. Discussion started: 19 June 2026


calcifying fluid $DIC_{cf}$ and $pH_{cf}$. Corals with higher $pH_{cf}$ (about 8.5) and lower $DIC_{cf}$ values (about 3500 µmol $kg^{-1}$) display $\Delta^7L_{iseep-CTRL}$ close to 0‰. Together these results support a close link between the physiological regulation of $pH_{cf}$, seawater pH, and the Li isotopic composition of coral skeletons.

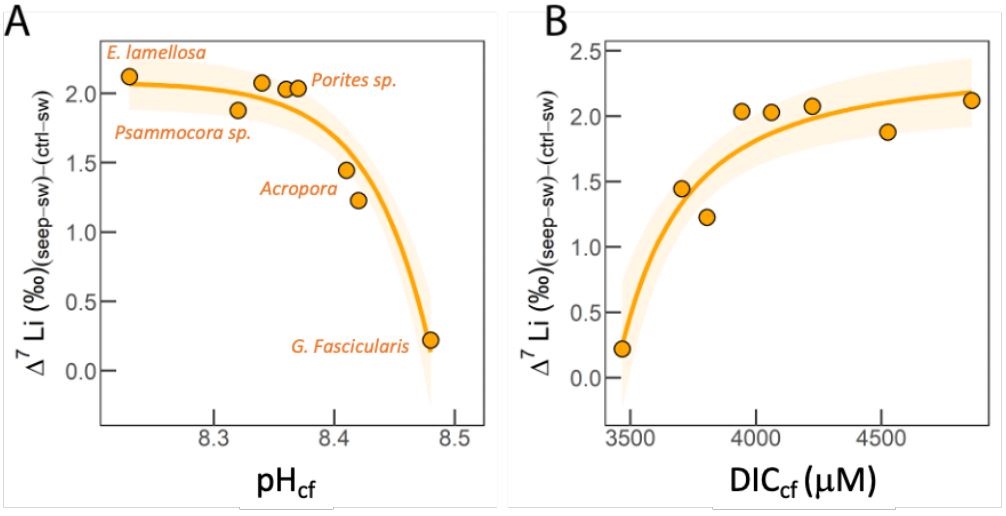


**Figure 8:** $\Delta^7Li_{seep-CTRL}$ as a function of $pH_{cf}$ (**A**) and $DIC_{cf}$ (**B**) of corals living under high $pCO_2$ seawater (seep). Orange lines represent the exponential fits, and the shadow orange zones, the confidence intervals.

### 4.4. Causes of a limited pH increase in the calcifying fluids

Boron geochemistry has shown that some species are unable to maintain elevated pH under acidic conditions, although the physiological mechanisms underlying this response remain poorly known. The close relationship between $pH_{cf}$ and lithium isotopic signatures strongly suggests that the physiological mechanisms acting to upregulate $pH_{cf}$ (and $DIC_{cf}$) are responsible for the observed enrichment of the lighter lithium isotope ($^6Li$) in coral skeletons. This can be explained through an integrated understanding of coral biology and Li transport mechanisms.

https://doi.org/10.5194/egusphere-2026-3326
Preprint. Discussion started: 19 June 2026


Intracellular pH regulation in coral cells is governed by a combination of intracellular chemical reactions and transmembrane transport of protons ($H^+$) or bicarbonate ions ($HCO_3^-$). Several transmembrane transporters are involved in pH regulation, including $Cl^-/HCO_3^-$ exchangers, $Na^+/HCO_3^-$ symporters, $Na^+/H^+$ antiporters (NHEs), and various ATPases that facilitate the movement of protons into or out of the cell or intracellular compartments. All these transporters have been identified in corals (Al-Moghrabi et al. 1996; Bhattacharya et al. 2016; Capasso et al. 2021) (Fig. 1 and Fig. S1). Experimental evidence from genetically modified cells has shown that NHE transporters efficiently transport lithium ions ($Li^+$) from the external medium into the intracellular cytoplasm (Pedersen & Counillon 2019). Although direct measurements of lithium transport through these transporters are lacking in corals, NHE and $Na^+/Ca^{2+}$ exchangers are widespread in animal cells, supporting their relevance for coral ion regulation.

During calcification, precipitation of calcium carbonate ($CaCO_3$) consumes $Ca^{2+}$ and $HCO_3^-$ while releasing protons into the calcifying fluid. To maintain elevated aragonite saturation in the calcifying fluid, corals must enhance the transport of $Ca^{2+}$ and dissolved inorganic carbon to the calcification site and efficiently remove excess protons. $Ca^{2+}$ can be transported into the calcifying fluid via $Ca^{2+}$ channels (Tambutte et al. 1996), $H^+/Ca^{2+}$ ATPases (Zoccola et al. 2004; Zoccola et al. 2015), and $Na^+/Ca^{2+}$ exchangers (Barron et al. 2018) (Fig. 1). Similar to NHEs, $Na^+/Ca^{2+}$ exchangers have been shown to transport $Li^+$ efficiently (Palty et al. 2004), which support a link between Li chemistry and the ion-transport associated with coral calcification. The excess protons produced during calcification are exported back into the calicoblastic cells through $Ca^{2+}$-ATPase, and the resulting cytoplasmic acidification is counteracted by the aforementioned transporters, including NHEs, which utilize $Li^+$ and $Na^+$ as counter-ions.

https://doi.org/10.5194/egusphere-2026-3326
Preprint. Discussion started: 19 June 2026


Overall, maintaining elevated calcification rates under low external pH conditions requires enhanced activity of several transporters involved in $H^+$, $HCO_3^-$, $Ca^{2+}$, $Na^+$, and $Li^+$ exchange. Several experimental studies have demonstrated that these transporters largely favor the kinetic transport of the lighter isotope, $^6Li$ (Poet et al. 2023, Thibon et al. 2021a; Vigier et al. 2015), in agreement with theoretical considerations for non-traditional (light) isotopes fractionation (e.g. Albarede 2004). This provides a potential mechanistic explanation for the isotopic patterns observed in figure 8 since increased transporters activity should result in negative isotopic fractionation (in favor of the $^6Li$) when the pH of the calcifying fluid ($pH_{cf}$) is high. This is consistent with both the vital effects established in section 4.1 and with the inverse relationship shown in Figure 9, indicating that decreasing $\Delta^7Li$ values relative to seawater are associated with increasing $pH_{cf}$.

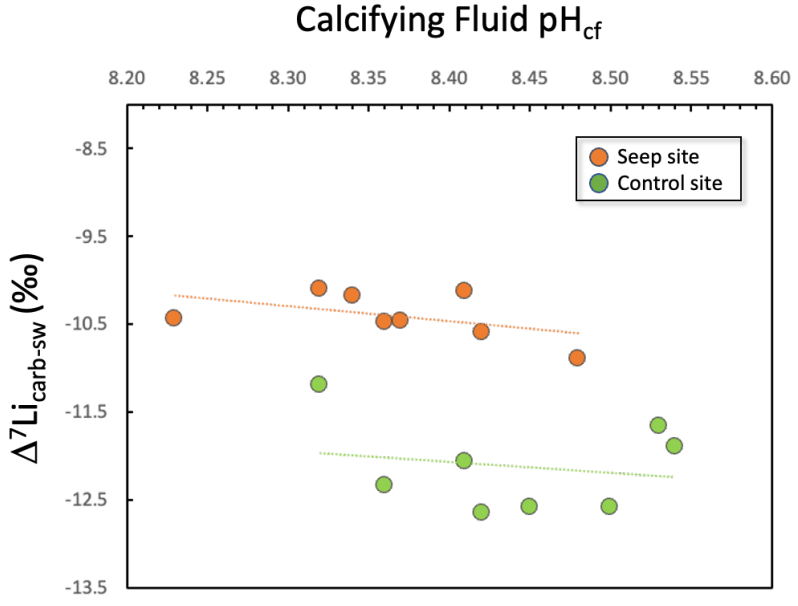


**Figure 9:** Li isotopic fractionation between seawater and coral skeleton as a function of pH of the calcifying fluid. $pH_{cf}$ was calculated on the total scale, and $DIC_{cf}$ is expressed in µmol $kg^{-1}$. Each circle represents a mean value for one coral species.

https://doi.org/10.5194/egusphere-2026-3326
Preprint. Discussion started: 19 June 2026


In addition, the isotopic difference between the two sites increases as the $pH_{cf}$ decreases (Fig. 8). Species capable of maintaining a high $pH_{cf}$ under lower seawater pH conditions, such as *G. fascicularis*, display similar isotopic fractionation in both control and seep conditions. In contrast, species living at the seeps site exhibit lower $pH_{cf}$ and a significant enrichment in heavy isotopes (up to 2‰) relative to control corals (e.g. *E. Lamellosa*). This suggests that low-pH conditions may reduce the efficiency of the ion-transport mechanisms involved in pH regulation, leading to weaker $^{6}Li$ enrichment and less efficient proton export.

Several experimental studies have shown that NHE isoforms respond to changes in pH, with their activity or expression significantly altered at low pH (Kapus et al. 1994; Wäge et al. 2015). In addition, proton gradients between the extracellular and intracellular environments influence ion-transport processes and NHE activity (Pedersen and Counillon 2019; Paris and Pouyssegur 1983). Under low seawater pH, elevated external $H^+$ concentrations may therefore reduce the efficiency of proton export from coral cells. Since NHEs transport $Li^+$ as a counter-ion to $H^+$, this may also explain the lack of Li enrichment observed in coral skeletons at the seep site ($Li_{carb\text{-}seep}$ = $Li\_{carb\text{-}control}$), despite slightly higher Li concentrations in the local seawater (see Section 4.1). Overall, these findings support the idea that coral responses to ocean acidification are linked to the capacity of corals to regulate their calcifying fluid chemistry caused by ion-transport processes associated with calcification.

## 5. Conclusion

In summary, lithium isotope systematics across a natural $CO_2$ gradient in Tutum Bay show that low seawater pH is associated with altered coral skeleton $\delta^{7}Li$ values and with changes in calcifying-fluid chemistry. The observed enrichment in $^{7}Li$ under low-pH conditions is

https://doi.org/10.5194/egusphere-2026-3326
Preprint. Discussion started: 19 June 2026


consistent with reduced $Na^+/H^+$ exchanger efficiency and, more broadly, with impaired ionic regulation during calcification. These results extend existing boron isotope constraints by linking carbonate chemistry to transporter-level physiology, and they indicate that $\delta^7Li$ can serve as a complementary tracer of coral responses to ocean acidification. More generally, this approach strengthens the use of lithium isotopes for resolving biogeochemical controls on carbonate-system behavior in modern and past environments.

## 6. Acknowledgements

We are grateful for access to facilities provided by the Oceanographic laboratory of Villefranche (LOV) and the Ecole Normale Supérieure de Lyon (ENSL, Philippe Télouk). This work benefited from the support of ANR ISO2MET (Project-ANR-18-CE34-0002) and ERC SEALi2Bio (#101097738). We are grateful to the population of Tutum Bay in Ambitle for allowing us to conduct the study on their reefs, and to the National Research Institute, the Milne Bay Provincial Research Committee, the New Ireland Provincial Administration, and the Conservation and Environment Protection Authority of Papua New Guinea for permits. We are indebted with Prof. Ralph Mana (University of UPNG) and to Prof. Katharina Fabricius (AIMS) for their invaluable help during the CARIOCA project. Thanks to the crew of the R/V Alis for their support during the cruise.

## 7. Fundings

This work was supported by the ANR [ISO2MET project, ANR-18-CE34-0002] and the ERC Advanced [SeaLi2Bio project, #101097738]. MTM was supported by an ARC Laureate Fellowship (LF120100049); SC was supported by an ARC DECRA (DE160100668). Sampling at

https://doi.org/10.5194/egusphere-2026-3326
Preprint. Discussion started: 19 June 2026


the PNG study site was partially funded by the French National Research Agency (ANR; project CARIOCA, ANR-15-CE02-0006-01, to RR-M), and by the Flotte Océanographique Française for using the research vessel Alis.

## 8. Data

The datasets supporting this article are available in the supporting information, and figures during peer review, and will be deposited at the time of the acceptance through the PANGEA database service and following FAIR principles.

## 9. Competing interests

The authors declare no competing interests.

## 10. CRediT

**NV**: Conceptualization, Supervision, Funding acquisition, Project administration, Writing - review & editing. **FT**: Methodology, Validation, Investigation, Formal analysis, Visualization, Writing - original draft, Writing - review & editing. **RRM**: Resources, Supervision, Writing - review & editing. **MM, PT**: Methodology, Validation. **AJ, LC, MP**: Writing - review & editing. **MMc**: Resources, Writing - review & editing. **CT**: Methodology, Validation, Formal analysis, Writing - review & editing. **SC**: Conceptualization, Project administration, Writing - review & editing.

https://doi.org/10.5194/egusphere-2026-3326
Preprint. Discussion started: 19 June 2026


## REFERENCES

Albarede F. (2004) Analytical Methods for Non-Traditional Isotopes. *Reviews in Mineralogy & Geochemistry* 55:113-152.

Al-Moghrabi, S., C. Goiran, D. Allemand, et al. (1996) Inorganic carbon uptake for photosynthesis bsy the symbiotic coral-dinoflagellate association II. Mechanisms for bicarbonate uptake. *Journal of Experimental Marine Biology and Ecology* 199(2): 227–48.

Balter, V., N. Vigier. (2014) Natural variations of lithium isotopes in a mammalian model. *Metallomics* 6(3): 582–6.

Barron, M.E., A.B. Thies, J.A. Espinoza, et al. (2018) A vesicular $Na^+/Ca^{2+}$ exchanger in coral calcifying cells. *PLOS ONE* 13(10): e0205367.

Bastian, L., N. Vigier, Y. Bouret, et al. (2018) Biological fractionation of lithium isotopes by cellular $Na^+/H^+$ exchangers unravels fundamental transport mechanisms. *Geostandards and Geoanalytical Research* 42(3): 403–15.

Bell, J.J., M. Shaffer, H.M. Luter, et al. (2022) Phototrophic sponge productivity may not be enhanced in a high $CO_2$ world. *Global Change Biology* 28(16): 4900–11.

Bhattacharya, D., S. Agrawal, M. Aranda, et al. (2016) Comparative genomics explains the evolutionary success of reef-forming corals. *eLife* 5: e13288.

Biscéré, T., M. Zampighi, A. Lorrain, et al. (2019) High $pCO_2$ promotes coral primary production. *Biology Letters* 15(7): 20180777.

Burton, K. W., & N. Vigier. (2011) Lithium isotopes as tracers in marine and terrestrial environments. In *Handbook of Environmental Isotope Geochemistry* 1, 41–60. Springer-Verlag. doi: 10.1007/978-3-642-10637-8_4

Capasso, L., P. Ganot, V. Planas-Bielsa, S. Tambutté, D. Zoccola. (2021) Intracellular pH regulation: characterization and functional investigation of $H^+$ transporters in *Stylophora pistillata*. *BMC Molecular and Cell Biology* 22(1): 18.

Case, D.H., L.F. Robinson, M.E. Auro, A.C. Gagnon. (2010) Environmental and biological controls on Mg and Li in deep-sea scleractinian corals. *Earth and Planetary Science Letters* 300(3): 215–25.

https://doi.org/10.5194/egusphere-2026-3326
Preprint. Discussion started: 19 June 2026


Chen, D., F. Thibon, A. Felbacq, et al. (2023) Coupled survey of lithium isotopes and Li/Ca in biogenic and inorganic carbonates. *Earth-Science Reviews* 244: 104500.

Clarke, H., J.P. D'Olivo, J. Falter, et al. (2017) Differential response of corals to regional mass-warming events as evident from skeletal Sr/Ca and Mg/Ca ratios. *Geochemistry, Geophysics, Geosystems* 18(5): 1794–809.

Comeau, S., P. J. Edmunds, N. B. Spindel, and R. C. Carpenter. (2013) The responses of eight coral reef calcifiers to increasing partial pressure of $CO_2$ do not exhibit a tipping point. *Limnol. Oceanogr.* 58: 388–398. https://doi.org/10.4319/lo.2013.58.1.0388

Comeau, S., C.E. Cornwall, M.T. McCulloch. (2017) Decoupling between the response of coral calcifying fluid pH and calcification to ocean acidification. *Scientific Reports* 7(1): 7573.

Comeau, S., C.E. Cornwall, T. Shlesinger, et al. (2022) pH variability at volcanic $CO_2$ seeps regulates coral calcifying fluid chemistry. *Global Change Biology* 28(8): 2751–63.

Cuny-Guirriec, K., E. Douville, S. Reynaud, et al. (2019) Coral Li/Mg thermometry: Caveats and constraints. *Chemical Geology* 523: 162–78.

D'Olivo, J.P., D.J. Sinclair, K. Rankenburg, M.T. McCulloch. (2018) A universal multi-trace element calibration for reconstructing sea surface temperatures from long-lived *Porites* corals: Removing 'vital-effects'. *Geochimica et Cosmochimica Acta* 239: 109–35.

Dellinger, M., A.J. West, G. Paris, et al. (2018) The Li isotope composition of marine biogenic carbonates: Patterns and mechanisms. *Geochimica et Cosmochimica Acta* 236: 315–35.

Dissard, D., E. Douville, S. Reynaud, et al. (2012) Light and temperature effects on $\delta^{11}B$ and B/Ca ratios of the zooxanthellate coral *Acropora* sp.: results from culturing experiments. *Biogeosciences* 9(11): 4589–605.

Douville, E., M. Paterne, G. Cabioch, et al. (2010) Abrupt sea surface pH change at the end of the Younger Dryas in the central sub-equatorial Pacific inferred from boron isotope abundance in corals (*Porites*). *Biogeosciences* 7(8): 2445–59.

Fabricius, K. E., C. Langdon, S. Uthicke, et al. (2011) Losers and winners in coral reefs acclimatized to elevated carbon dioxide concentrations. *Nature Climate Change* 1(3): 165–169.

Fallon, S.J., M.T. McCulloch, C. Alibert. (2003) Examining water temperature proxies in *Porites* corals from the Great Barrier Reef: a cross-shelf comparison. *Coral Reefs* 22(4): 389–404.

https://doi.org/10.5194/egusphere-2026-3326
Preprint. Discussion started: 19 June 2026


Foster, G.L., J.W.B. Rae. (2016) Reconstructing Ocean pH with Boron Isotopes in Foraminifera. *Annual Review of Earth and Planetary Sciences* 44(1): 207–37.

Foster, G.L., P.A.E.P. von Strandmann, J.W.B. Rae. (2010) Boron and magnesium isotopic composition of seawater. *Geochemistry, Geophysics, Geosystems* 11(8).

Fowell, S.E., K. Sandford, J.A. Stewart, et al. (2016) Intrareef variations in Li/Mg and Sr/Ca sea surface temperature proxies in the Caribbean reef-building coral *Siderastrea siderea*. *Paleoceanography* 31(10): 1315–29.

Geissler, L., V. Meunier, N. Rädecker, et al. (2021) Highly Variable and Non-complex Diazotroph Communities in Corals From Ambient and High $CO_2$ Environments. *Frontiers in Marine Science* 8.

Guillermic, M., L.P. Cameron, I. De Corte, et al. (2021) Thermal stress reduces pocilloporid coral resilience to ocean acidification by impairing control over calcifying fluid chemistry. *Science Advances* 7(2): eaba9958.

Holcomb, M., A.A. Venn, E. Tambutté, et al. (2014) Coral calcifying fluid pH dictates response to ocean acidification. *Scientific Reports* 4(1): 5207.

Hoegh-Guldberg, O., E. S. Poloczanska, W. Skirving & S. Dove. (2017) Coral reef ecosystems under climate change and ocean acidification. *Frontiers in Marine Science* 4. https://doi.org/10.3389/fmars.2017.00158

Jouini, A., L. Payant, N. Vigier. (2026) Advances in high-precision lithium isotopic measurements with the Neoma™ MC-ICP-MS. *J. Anal. At. Spectrom.* 41: 1004-1016. doi:10.1039/D5JA00426H

Kapus, A., S. Grinstein, S. Wasan, et al. (1994) Functional characterization of three isoforms of the $Na^+/H^+$ exchanger stably expressed in Chinese hamster ovary cells. *The Journal of Biological Chemistry* 269(38): 23544–52.

Klochko, K., A.J. Kaufman, W. Yao, R.H. Byrne, J.A. Tossell. (2006) Experimental measurement of boron isotope fractionation in seawater. *Earth and Planetary Science Letters* 248(1): 276–85.

Marriott, C.S., G.M. Henderson, N.S. Belshaw, A.W. Tudhope. (2004a) Temperature dependence of $\delta^7$Li, $\delta^{44}$Ca and Li/Ca during growth of calcium carbonate. *Earth and Planetary Science Letters* 222(2).

https://doi.org/10.5194/egusphere-2026-3326
Preprint. Discussion started: 19 June 2026


Marriott, C.S., G.M. Henderson, R. Crompton, et al. (2004b) Effect of mineralogy, salinity, and temperature on Li/Ca and Li isotope composition of calcium carbonate. *Chemical Geology* 212(1): 5–15.

McCulloch, M. T., J. P. D'Olivo, J. Falter, et al. (2017) Coral calcification in a changing World and the interactive dynamics of pH and DIC upregulation. *Nature Communications* 8: 15686. doi:10.1038/ncomms15686

Meunier, V., L. Geissler, S. Bonnet, et al. (2021) Microbes support enhanced nitrogen requirements of coral holobionts in a high $CO_2$ environment. *Molecular Ecology* 30(22): 5888–99.

Mitsuguchi, T., E. Matsumoto, O. Abe, et al. (1996) Mg/Ca Thermometry in Coral Skeletons. *Science* 274(5289): 961–3.

Montagna, P., M. McCulloch, E. Douville, et al. (2014) Li/Mg systematics in scleractinian corals: Calibration of the thermometer. *Geochimica et Cosmochimica Acta* 132: 288–310.

Okazaki, R. R., E. K. Towle, R. van Hooidonk, et al. (2017) Species-specific responses to climate change and community composition determine future calcification rates of Florida Keys reefs. *Global Change Biology* 23: 1023–1035. https://doi.org/10.1111/gcb.13481

Orr, J.C., V.J. Fabry, O. Aumont, et al. (2005) Anthropogenic ocean acidification over the twenty-first century and its impact on calcifying organisms. *Nature* 437(7059): 681–6.

Palty, R., E. Ohana, M. Hershfinkel, et al. (2004) Lithium-Calcium Exchange Is Mediated by a Distinct Potassium-independent Sodium-Calcium Exchanger. *Journal of Biological Chemistry* 279(24): 25234–40.

Paris, S., J. Pouysségur. (1983) Biochemical characterization of the amiloride-sensitive $Na^+/H^+$ antiport in Chinese hamster lung fibroblasts. *J. Biol. Chem.* 258(6): 3503–8.

Pedersen, S.F., L. Counillon. (2019) The SLC9A-C Mammalian $Na^+/H^+$ Exchanger Family: Molecules, Mechanisms, and Physiology. *Physiol Rev* 99(4): 2015–113.

Pichler, T., T. Biscéré, J. Kinch, et al. (2019) Suitability of the shallow water hydrothermal system at Ambitle Island (Papua New Guinea) to study the effect of high $pCO_2$ on coral reefs. *Marine Pollution Bulletin* 138: 148–58.

Pichler, T., J. Veizer, G.E.M. Hall. (1999) The chemical composition of shallow-water hydrothermal fluids in Tutum Bay, Ambitle Island, Papua New Guinea and their effect on ambient seawater. *Marine Chemistry* 64(3): 229–52.

https://doi.org/10.5194/egusphere-2026-3326
Preprint. Discussion started: 19 June 2026


Poet, M., N. Vigier, Y. Bouret, G. Jarretou, et al. (2023) Biological fractionation of lithium isotopes by cellular $Na^+/H^+$ exchangers unravels fundamental transport mechanisms. *iScience* 26: 106887.

Quinn, T.M., D.E. Sampson. (2002) A multiproxy approach to reconstructing sea surface conditions using coral skeleton geochemistry. *Paleoceanography* 17(4): 14-1–14-11.

R Core Team. (2017) *R: A language and environment for statistical computing*. R Foundation for Statistical Computing, Vienna, Austria.

Rollion-Bard, C., D. Blamart. (2015) Possible controls on Li, Na, and Mg incorporation into aragonite coral skeletons. *Chemical Geology* 396: 98–111. https://doi.org/10.1016/j.chemgeo.2014.12.011

Rollion-Bard, C., N. Vigier, A. Meibom, et al. (2009) Effect of environmental conditions and skeletal ultrastructure on the Li isotopic composition of scleractinian corals. *Earth and Planetary Science Letters* 286(1–2): 63–70.

Rodolfo-Metalpa, R. (2018. *CARIOCA 3 cruise, Alis R/V*.

Stewart, J.A., L.F. Robinson, R.D. Day, et al. (2020) Refining trace metal temperature proxies in cold-water scleractinian and stylasterid corals. *Earth and Planetary Science Letters* 545: 116412.

Tambutté, É., D. Allemand, E. Mueller, J. Jaubert. (1996) A compartmental approach to the mechanism of calcification in hermatypic corals. *Journal of Experimental Biology* 199(5): 1029–41.

Thibon, F., J. Goedert, N. Séon, L. et al. (2022) The ecology of modern and fossil vertebrates revisited by lithium isotopes. *Earth and Planetary Science Letters* 599: 117840.

Thibon, F., L. Weppe, N. Vigier, C. Churlaud, et al. (2021a) Large-scale survey of lithium concentrations in marine organisms. *Science of The Total Environment* 751: 1453.

Thibon, F., L. Weppe, M. Montanes, et al. (2021b) Lithium isotopic composition of reference materials of biological origin TORT-2, DORM-2, TORT-3, DORM-4, SRM-1400 and ERM-CE278k. *J Anal At Spectrom* 36(7): 1381–8.

Thibon, F., M. Metian, F. Oberhansli, et al. (2021c) Bioaccumulation of lithium isotopes in mussel soft tissues and implications for coastal environments. *ACS Earth and Space Chemistry* 5(6): 1407–17.

https://doi.org/10.5194/egusphere-2026-3326
Preprint. Discussion started: 19 June 2026


Trotter, J., P. Montagna, M. McCulloch, et al. (2011) Quantifying the pH 'vital effect' in the temperate zooxanthellate coral *Cladocora caespitosa*: Validation of the boron seawater pH proxy. *Earth and Planetary Science Letters* 303(3): 163–73.

Venn, A. A., E. Tambutté, M. Holcomb, et al. (2013) Impact of seawater acidification on pH at the tissue–skeleton interface and calcification in reef corals. *PNAS* 110: 1634–1639. doi:10.1073/pnas.1216153110

Venn, A.A., E. Tambutté, S. Comeau, S. Tambutté. (2022) Proton gradients across the coral calcifying cell layer: Effects of light, ocean acidification and carbonate chemistry. *Frontiers in Marine Science* 9.

Verney-Carron, A., N. Vigier, et al. (2015) Lithium isotopes in hydrothermally altered basalts from Hengill 1 (SW Iceland). *Earth Planet. Sci. Lett.* 411: 62-71.

Vigier, N., A. Decarreau, R. Millot, et al. (2008). Quantifying Li isotope fractionation during smectite formation and implications for the Li cycle. *Geochimica et Cosmochimica Acta* 72(3): 780–92.

Vigier, N., C. Rollion-Bard, Y. Levenson, J. Erez. (2015) Lithium isotopes in foraminifera shells as a novel proxy for the ocean dissolved inorganic carbon (DIC). *Comptes Rendus Geoscience* 347(1): 43–51.

Wäge, J., J.D. Hardege, T.A. Larsson, et al. (2015) Effects of low seawater pH on the marine polychaete *Platynereis dumerilii*. *Marine Pollution Bulletin* 95(1): 166–72.

Zeebe, R.E., D. Wolf-Gladrow. 2001. *$CO_2$ in Seawater: Equilibrium, Kinetics, Isotopes.* Gulf Professional Publishing. 382 p.

Zoccola, D., E. Tambutté, E. Kulhanek, et al. (2004) Molecular cloning and localization of a PMCA P-type calcium ATPase from the coral *Stylophora pistillata*. *Biochimica et Biophysica Acta (BBA) - Biomembranes* 1663(1): 117–26.